Fingerprints of the nodal structure of autoionizing vibrational wave functions in clusters: Interatomic Coulombic decay in Ne dimer

Nimrod Moiseyev, Robin Santra, Jürgen Zobeley, and Lorenz S. Cederbaum

Articles you may be interested in

Fingerprints of the nodal structure of autoionizing vibrational wave functions in clusters: Interatomic Coulombic decay in Ne dimer

Nimrod Moiseyev
Department of Chemistry and Minerva Center of Nonlinear Physics in Complex Systems,
Technion—Israel Institute of Technology, Haifa 32000, Israel

Robin Santra,[a] Jürgen Zobeley, and Lorenz S. Cederbaum
Theoretische Chemie, Physikalisch-Chemisches Institut, Universität Heidelberg, Im Neuenheimer Feld 229,
D-69120 Heidelberg, Germany

The removal of an inner-valence electron from neutral neon clusters leads to autoionization and subsequent fragmentation of the cationic clusters in accordance with the interatomic Coulombic decay mechanism discovered recently. Using non-Hermitian quantum scattering theory we investigate this process in detail for the Ne dimer. We show that a pronounced structure can be observed when measuring the autoionizing electron or the Ne^+ kinetic energy distributions. This phenomenon is associated with the properties of the vibrational autoionizing resonance states of the electronically excited cationic dimer. By suppressing coherence among the different vibrational autoionizing resonances, or by selectively exciting one of them, the structures in the kinetic energy distributions become more pronounced. It is demonstrated that these structures reflect the nodal structure of the wave functions of the autoionizing vibrational states most populated by the initial ionization of the neutral neon dimer. In a coherent decay we encounter substantial interference effects, but the nodal pattern of the corresponding wave functions is still present. The kinetic energy distributions are generally very sensitive to details of the potential energy curves of clusters. © *2001 American Institute of Physics.* [DOI: 10.1063/1.1361070]

I. INTERATOMIC COULOMBIC DECAY IN CLUSTERS

Resonance states are states at which the system has sufficient energy to break up into subsystems. The lifetime of the state strongly depends on the system and the mechanism which leads to the decay process. In the Auger process[1] the electron decay results from electron correlation between core shell electrons and valence electrons. By exciting or ionizing a core shell electron we produce a hole in the inner shell. The transition of another electron into this hole releases energy which is sufficient for ionization of a valence shell electron. Let us consider a weakly bound cluster, consisting of rare gas atoms, for instance. Does the Auger process depend on the cluster environment of the initially core-ionized atom? In principle the answer is yes, but the influence of neighboring atoms on the decay rate must be expected to be very small. Core electron orbitals are very compact and consequently the interatomic core–valence electron correlation in clusters is very weak.

Cederbaum and co-workers[2,3] were the first to realize that the interatomic electron correlation in clusters can be highly increased if an electron is excited from an inner-valence orbital rather than from a core orbital. This is due to the larger spatial extension of the valence shell orbital as compared to the compact core orbital. One system where such a phenomenon can be observed is the neon dimer.[4] Although the energy of $Ne^+(2s)$ is *below* the ground state

energy of the dication, Ne^{2+}, the total energy of $Ne^+(2s)$ *together* with the energy of the noninteracting neutral atom, $Ne+Ne^+(2s)$, is *above* the ground state energy of the doubly ionized cluster, Ne_2^{2+}. This is due to the drop of the double ionization threshold of Ne_2, which reflects the fact that the two positive charges are not localized at a single atomic center but equally distributed over the two spatially separated neon sites. The repulsion of the two positive charges leads to a Coulombic explosion of Ne_2^{2+} resulting in two Ne^+ fragments. This configuration of a dimer with two positive charges equally distributed over the two spatially separated neon sites is the outcome of the autoionization process of the cationic dimer $Ne_2^+(2s)$.

In this paper we will show that the Coulombic explosion of the cationic neon dimer due to the interatomic Coulombic decay (ICD),[5] leads to a remarkable structure in the kinetic energy distributions of the autoionizing electron and of the dissociated neon cations. This structure is a magnified mapping of the spatial structure of the autoionizing vibrational cluster wave function of $Ne_2^+(2s)$ onto the energy space of the free electron and/or Ne^+.

II. COMPLEX POTENTIAL ENERGY SURFACE OF $Ne_2^+(2s)$ AND POTENTIAL SURFACES FOR Ne_2 AND Ne_2^{2+}

As a basic requirement for the dynamical studies on the electronic decay of the Ne_2^+ inner-valence states, the involved potential energy surfaces have to be determined. The

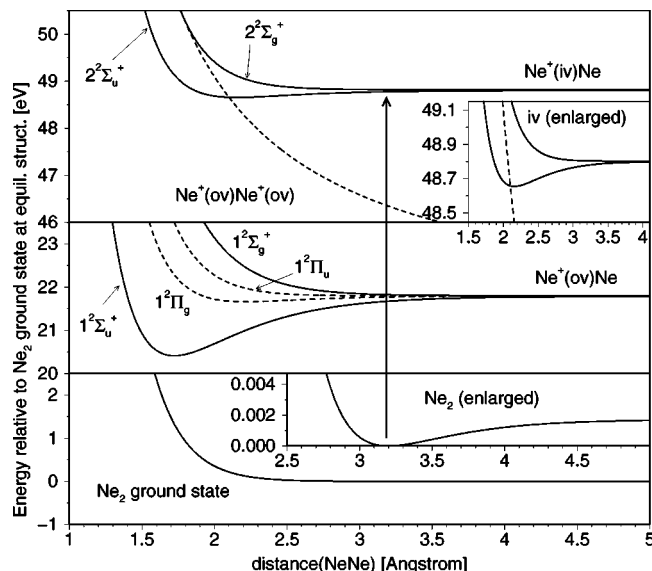[a]Electronic mail: robin.santra@tc.pci.uni-heidelberg.de

FIG. 1. Potential energy surfaces of the electronic ground state of the neon dimer, the outer- and inner-valence states of Ne_2^+, and the two-site outer-valence states of Ne_2^{2+}. Since these dicationic states are all very similar to each other, only one is shown. By inner-valence ionization the vibrational ground state wave function of Ne_2 is lifted up to the $2\,^2\Sigma_u^+$ and $2\,^2\Sigma_g^+$ surfaces of Ne_2^+. For most interatomic distances the dicationic two-site surfaces are *lower* in energy than the inner-valence surfaces, giving rise to an efficient interatomic electronic decay (ICD). The striking difference between the highly repulsive dicationic surfaces and the rather flat neutral and inner-valence surfaces leads to remarkable dynamical effects in the kinetic energy spectrum of the emitted ICD electron.

relevant valence cationic and dicationic potential energy surfaces of the Ne_2 system, as well as the neutral ground state surface, are presented in Fig. 1. The surfaces of the cationic and dicationic states were calculated within the framework of Green's function methods, using the algebraic diagrammatic construction scheme (ADC). The ADC-Green's function methods have been discussed in detail in the literature.[6–9] We therefore only mention that the ADC(n) scheme represents a sophisticated many-body perturbation theoretical expansion of the Green's function under consideration, which is complete up to nth order but includes additional classes of contributions up to infinite order. The obtained results are size consistent in any order of perturbation theory. The ADC(3) scheme of the one-particle Green's function (extended 2ph-TDA) and the ADC(2) scheme for the particle–particle propagator have been used, respectively, to calculate the Ne_2^+ and Ne_2^{2+} states in the valence energy region. The orbital energies and Coulomb integrals resulting from a Hartree–Fock calculation of the neutral ground state serve as input for the ADC calculations. The Hartree–Fock calculation was performed with the *ab initio* program package GAMESS-UK[10] using the d-aug-cc-pVTZ Gaussian basis set.[11] The neutral ground state surface of Ne_2 has been taken from highly accurate *ab initio* data published recently.[12]

Due to the weak van der Waals interaction, which is typical for rare gas systems, the neutral ground state surface of Ne_2 has a very shallow minimum at about 3.2 Å with only two vibrational bound states. The four outer-valence (ov) cationic potential surfaces Ne_2^+(ov), resulting from removal

of one electron out of a $Ne(2p)$-type orbital, are bound states with respect to electron emission. The two lower lying $1\,^2\Sigma_u^+$ and the $1\,^2\Pi_g$ states possess distinct minima, whereas the higher lying $1\,^2\Pi_u$ and $1\,^2\Sigma_g^+$ states are purely repulsive. These results are in good agreement with corresponding data in the literature.[13]

In contrast to the outer-valence cationic states and also in sharp contrast to the situation in the isolated Ne atom, the two inner-valence (iv) cationic states Ne_2^+(iv), resulting from removal of one electron out of a $Ne(2s)$-type orbital, are electronic resonances over a wide range of Ne–Ne interatomic distances. Both states, the $2\,^2\Sigma_u^+$ as well as the $2\,^2\Sigma_g^+$ state, can undergo electron emission resulting in outer-valence dicationic states having one vacancy on each of the two Ne atoms (''two-site'' states). It is an essential point to notice that, because of the reduced Coulombic interaction of the two vacancies being localized on different Ne atoms, only the ''two-site'' states lie energetically lower than the two inner-valence cationic states. The Ne_2^{2+} ''one-site'' states with both vacancies being localized on the same Ne atom are much higher in energy (≈ 61 eV), and are, therefore, like the dicationic states in the isolated Ne atom, not accessible for an electronic decay of the inner-valence cationic states. The decay mechanism of an inner-valence hole in the Ne_2 system is therefore of purely interatomic nature (ICD), as opposed to Auger decay of a core hole.

The inner-valence $2\,^2\Sigma_u^+$ surface has a distinct energy minimum at about 2.2 Å, supporting 11 vibrational bound states, whereas the $2\,^2\Sigma_g^+$ surface is purely repulsive or rather has a very shallow minimum with a single vibrational bound state at the interatomic distance corresponding to the minimum position of the neutral ground state surface. The latter finding is still a matter of discussion.[13]

The presence of 6 electrons of $2p$ type in Ne leads to 12 Ne_2^{2+} two-site states. The respective surfaces are purely repulsive because of the Coulombic interaction of the two positive charges on the two Ne atoms. These surfaces intersect the inner-valence $2\,^2\Sigma_u^+$ surface at about 2.1 Å, which means that the latter state becomes electronically stable at Ne–Ne distances smaller than 2.1 Å. In order to simplify the dynamical model studies we have replaced the 12 dicationic surfaces, which are very similar to each other, by an averaged single surface (see Fig. 1).

In the following dynamics investigation we will focus on the electronic decay of the $2\,^2\Sigma_u^+$ state of Ne_2^+ only, which supports several vibrational bound states. In our study the $2\,^2\Sigma_u^+$ state is populated via ionization out of the vibrational ground state of the neutral Ne_2 system. Due to the shallow energy minimum and the small curvature of the Ne_2 surface the starting wave packet is represented by a relatively broad Gaussian-type wave packet. In this context it should be noted that, because of the very small separation of the two inner-valence Ne_2^+ states at the equilibrium distance of the neutral Ne_2, it might be hardly possible to populate only the $2\,^2\Sigma_u^+$ state in a direct photoionization experiment starting from the neutral ground state. However, it should be possible, at least in principle, to populate the $2\,^2\Sigma_u^+$ state exclusively by a resonant excitation out of, e.g., the $1\,^2\Pi_g$ outer-valence state
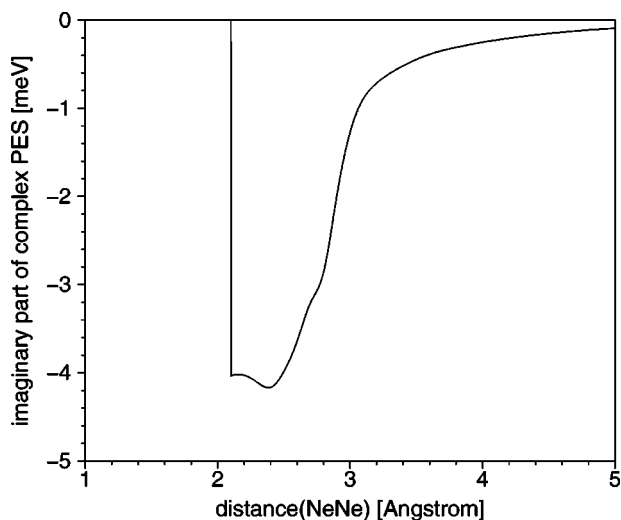
FIG. 2. Imaginary part of the complex potential energy surface of the $2\,{}^2\Sigma_u^+$ inner-valence state of Ne_2^+, as a function of the interatomic distance. This quantity is directly related to the local electronic decay width $\Gamma[2\,{}^2\Sigma_u^+ Ne_2^+](R)$. Results were obtained by means of the complex-absorbing-potential method (Refs. 14 and 15). At 2.1 Å the $2\,{}^2\Sigma_u^+$ surface passes the double ionization threshold (see Fig. 1). Below this point the local decay width vanishes.

following outer-valence ionization of the neutral ground state.

Calculation of the imaginary part of the complex potential energy surface of the $2\,{}^2\Sigma_u^+$ state was carried out by means of the CAP/CI method,[14,15] an implementation of a complex absorbing potential (CAP)[16] at the configuration interaction (CI) level.[17] This approach is ideally suited to take care of the nontrivial electron scattering problem, which is otherwise not directly amenable to standard quantum chemistry techniques like Gaussian basis set expansions. Furthermore, the strong coupling between electronic configurations associated with electronic decay processes is dealt with in an appropriate manner.

We computed molecular orbitals, i.e., Hartree–Fock one-particle states, for the electronic ground state of Ne_2 employing a Gaussian basis set that we constructed by adding a set of diffuse functions $(1s,1p,1d,1f)$ to d-aug-cc-pVTZ. The many-electron configuration space of the dimer cation was spanned by all one-hole configurations which result from removing one electron from the different valence orbitals, as well as by all single and double excitations of these references that are compatible with the frozen-core approximation and an active space consisting of all orbitals which are occupied in the Hartree–Fock ground state determinant. The absorbing potential was chosen in accordance with the one given in Ref. 15. From the spectrum of the complex symmetric CAP/CI matrix obtained in this way we extracted the complex Siegert energy of the electronic resonance.

The imaginary part of the complex potential energy curve $E[2\,{}^2\Sigma_u^+ Ne_2^+](R)$ is depicted in Fig. 2 as a function of the interatomic distance R. This quantity is proportional to the local electronic decay width,

$$\Gamma[2\,{}^2\Sigma_u^+ Ne_2^+](R) = -2\,\mathrm{Im}\,E[2\,{}^2\Sigma_u^+ Ne_2^+](R). \qquad (1)$$

As we have shown previously (see Fig. 1), the cationic inner valence state of u symmetry is bound for interatomic distances smaller than 2.1 Å. Therefore the imaginary part of its complex potential energy curve vanishes below this distance. It is interesting to note that $\mathrm{Im}\,E[2\,{}^2\Sigma_u^+ Ne_2^+](R)$ is discontinuous at the electron detachment threshold. Such a behavior in the presence of an attractive Coulomb potential is well known.[18,19] Short-range and repulsive Coulomb potentials, however, which do not possess Rydberg-type eigenstates, show a continuous threshold behavior. At large interatomic distances the ICD electron emission rate tends to zero, because the energy transfer probability between $Ne^+(2s)$ and Ne, which underlies the interatomic Coulombic decay mechanism, decreases. In the range of distances that are of relevance in the present context, the decay widths are of the order of 1 meV, corresponding to lifetimes of several hundred femtoseconds. At the equilibrium geometry of the ground state of Ne_2 (3.2 Å) the lifetime is about 530 fs. This time scale turns out to be comparable to that of the nuclear dynamics on the relatively flat inner-valence potential energy surface. Relaxation by photon emission may be neglected here since the fluorescence decay width of inner-valence excited neon is of the order of 1 μeV.[20]

We also calculated the local decay rate for the $2\,{}^2\Sigma_g^+$ state of Ne_2^+.[4] The lifetimes for this inner-valence state are comparable to those of the u-symmetry state reported previously. In the following we will not discuss the $2\,{}^2\Sigma_g^+$ state, which supports at most a single vibrational, Gaussian-shaped bound state. Our attention will be focused on the exciting effects exerted by vibrational wave functions with nodal structure.

III. ICD ELECTRON AND Ne$^+$ KINETIC ENERGY DISTRIBUTIONS BY NON-HERMITIAN QUANTUM SCATTERING THEORY

A. Formal aspects

In the ensuing sections a detailed investigation of ICD electron emission in inner-valence ionized neon dimer and the associated fragmentation process is carried out within the framework of non-Hermitian quantum scattering theory. This technique has been developed and has been used by Moiseyev and co-workers to explain the experimental results obtained in helium diffraction from corrugated copper surfaces, scattering intensity measurements of HD molecules from flat Ag and Pt surfaces, measurements of helium harmonic generation spectra, and of the cross sections obtained in electron scattering experiments from hydrogen molecules (see Refs. 21, 22, and references therein). First, let us motivate the use of non-Hermitian quantum scattering theory in place of the ''conventional'' (i.e., Hermitian) one.

The transition probability amplitude, $t(E)$, for a half-collision experiment, where the decaying state $|0\rangle$ and the final state $|f\rangle$ are in different electronic and vibrational states, is given by the Lippmann–Schwinger equation,[23]

$$t(E) = \langle 0|1 + \hat{G}\hat{V}|f\rangle = t_{\text{direct}}(E) + t_{\text{res}}(E). \tag{2}$$

$\hat{G} = \lim_{\eta \to 0^+}(E - \hat{H} + i\eta)^{-1}$ is the Green operator of the interacting target–projectile system. The decaying state $|0\rangle$ is associated with a wave packet which is expanded in the basis set of the eigenfunctions of $\hat{H}$. The interaction between target and projectile is mediated by the operator $\hat{V}$. The final state $|f\rangle$ is an eigenstate with energy E of the Hamiltonian $\hat{H}_f = \hat{H} - \hat{V}$, corresponding to the target and a separate, free projectile. To be specific, in this paper the projectile is the ICD electron and the target is Ne_2^{2+}.

The direct term $t_{\text{direct}}(E) = \langle 0|f\rangle$ can be neglected here, the indirect term, $t_{\text{res}}(E)$, is given by

$$t_{\text{res}}(E) = \lim_{\eta \to 0^+} \int d\epsilon\, \rho(\epsilon) \frac{\langle 0|\epsilon\rangle\langle\epsilon|\hat{V}|f\rangle}{E - \epsilon + i\eta}, \tag{3}$$

where $\hat{H}|\epsilon\rangle = \epsilon|\epsilon\rangle$, and $\rho(\epsilon)$ stands for the density of states. Typically, the resonance states provide the dominant contributions to $t(E)$. However, since in Hermitian quantum mechanics the eigenstates $|\epsilon\rangle$ are restricted to the Hermitian domain of $\hat{H}$, the eigenvalues ϵ assume real values only, and the information about a resonance phenomenon is spread over an infinite number of continuum states. Furthermore, this treatment is the reason why a direct application of the Born–Oppenheimer approximation is a delicate problem. Describing a resonance state by a simple product of electronic and nuclear wave functions would be permissible only if a given electronic potential energy surface were isolated. However, within the framework of Hermitian quantum mechanics, above the autoionization threshold there is a continuum of potential energy surfaces whose energy spacings are infinitesimal.

The situation can be remedied by observing that a resonance state is characterized by a simple pole of the Green operator, $E_n^{\text{res}} = \epsilon_n - (i/2)\Gamma_n$, located on the non-Hermitian sheet of the corresponding Riemann surface. E_n^{res} is a *complex* eigenvalue of the Hamiltonian $\hat{H}$, that is, $\hat{H}|n\rangle = E_n^{\text{res}}|n\rangle$, where $|n\rangle$ is an eigenstate which is *not* in the Hermitian domain of $\hat{H}$. By making use of complex scaling methods,[21] which are closely related to the introduction of a CAP in the Hamiltonian,[24] the Green operator is analytically continued onto the non-Hermitian sheet. This procedure turns the complex resonance poles E_n^{res} into eigenvalues of a non-Hermitian Hamilton operator, the associated eigenstates are rendered square integrable. Therefore, the use of non-Hermitian quantum scattering theory[21] enables us to concentrate the information about resonances into *discrete, square-integrable* states and to replace the integral in the expression for $t_{\text{res}}(E)$ by a sum over the discrete resonance states $|n\rangle$,

$$t_{\text{res}}(E) = \sum_n \frac{(0|n)(n|\hat{V}|f)}{E - E_n^{\text{res}}}. \tag{4}$$

Here, for the sake of simplicity and without loss of generality, the so called c product $(\cdot|\cdot)$ between two states is defined by $(f|g) := \langle f^*|g\rangle$. The c product is a generalized inner product (see Refs. 21, 25, and references therein). Its introduction is necessary because of the mathematical properties of non-Hermitian Hamilton operators. It is important to realize that this generalization of the inner product can give rise to interesting interference effects between resonance states. This observation played a key role in the explanation of the unexpectedly marked structure in the measured electron–H_2 scattering cross sections.[22,26]

Neglecting nonlocal effects,[19,27] threshold effects which we will say more about in the following, we can make the assumption that the electronic decay and subsequent fragmentation of the inner-valence ionized neon dimer proceeds via a *single electronic* resonance state, $2\,^2\Sigma_u^+$, involving a number of vibrational wave functions $\{\chi_v[2\,^2\Sigma_u^+Ne_2^+]\}$. The Born–Oppenheimer approximation can be invoked because the technique of analytic continuation allows a clean separation of adiabatic electronic resonance states and continuum scattering states in the complex energy plane. Thus the vibrational states $\chi_v[2\,^2\Sigma_u^+Ne_2^+]$ and the associated complex energies $E_v[2\,^2\Sigma_u^+Ne_2^+]$ are obtained by solving the non-Hermitian eigenvalue problem of the nuclear Hamiltonian

$$\hat{H}_{BO} = -\frac{\hbar^2}{2\mu_{Ne_2}} \frac{d^2}{dR^2} + E[2\,^2\Sigma_u^+Ne_2^+](R). \tag{5}$$

μ_{Ne_2} is the reduced mass of the neon–neon system. The complex, nuclear-dependent electronic energy $E[2\,^2\Sigma_u^+Ne_2^+](R)$, computed by using the ADC and CAP/CI methods (see Sec. II), serves as a potential energy in Eq. (5).

In order to use Eq. (4) to describe the kinetic energy distribution of the ICD electrons, we have to specify the decaying state $|0\rangle$. This state depends on its preparation. It can be prepared, for instance, by photon impact, and we assume that the conditions justifying the sudden approximation are fulfilled, i.e., that the incident photon energy is larger by several electron volts than the binding energy of the released photoelectron.[28] Then the interaction of the photoelectron with Ne_2^+ is small and may be disregarded. Owing to the fast ionization process, the nuclei have no time to move during the preparation, and $|0\rangle$ becomes a product of the $2\,^2\Sigma_u^+$ electronic wave function and the ground vibrational wave function, $\chi_0[Ne_2]$, of neon dimer.

Identifying the discrete resonance states $|n\rangle$ to be products of the $2\,^2\Sigma_u^+$ electronic wave function with vibrational states $\chi_v[2\,^2\Sigma_u^+Ne_2^+]$, we obtain from Eq. (4)

$$\sigma(E_{\text{kin}}) = \int dE_f[Ne_2^{2+}] \left| \sum_v^{\text{res}} \frac{(\chi_0[Ne_2]|\chi_v[2\,^2\Sigma_u^+Ne_2^+])_R (\chi_v[2\,^2\Sigma_u^+Ne_2^+]|\Gamma^{1/2}[2\,^2\Sigma_u^+Ne_2^+](R)|\chi_{E_f}[Ne_2^{2+}])_R}{E_{\text{kin}} + E_f[Ne_2^{2+}] - E_v[2\,^2\Sigma_u^+Ne_2^+]} \right|^2, \tag{6}$$
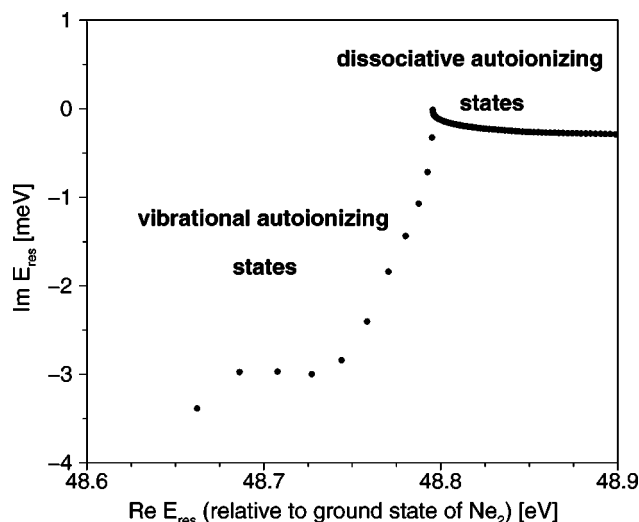
FIG. 3. The complex vibrational energies E_v of the decaying $2\,^2\Sigma_u^+$ electronic state of Ne_2^+. This electronic state supports 11 discrete vibrational autoionizing states below the dissociative autoionizing continuum. The lifetime of a vibrational autoionizing state is given by $\tau[\text{fs}] = -329/\text{Im}\,E_{\text{res}}[\text{meV}]$.

where the electronic states have all dropped out. A detailed account of the derivation of Eq. (6) can be found in the Appendix. The notation $(\cdot|\cdot)_R$ implies integration over the interatomic distance R. The states $\chi_{E_f}[Ne_2^{2+}]$ in Eq. (6) are the dissociative nuclear wave functions with energy $E_f[Ne_2^{2+}]$ of Ne_2^{2+} in its ground electronic state. The coupling of these to the vibrational resonance states $\chi_v[2\,^2\Sigma_u^+ Ne_2^+]$ is described by the matrix element $(\chi_v[2\,^2\Sigma_u^+ Ne_2^+]|\Gamma^{1/2}[2\,^2\Sigma_u^+ Ne_2^+](R)|\chi_{E_f}[Ne_2^{2+}])_R$, where a nuclear-dependent complex phase factor accompanying the square root of the local decay width $\Gamma[2\,^2\Sigma_u^+ Ne_2^+](R)$ has been neglected for simplicity. The integration over the Ne_2^{2+} energy in Eq. (6) takes into account all possible final states of the Ne^+ fragments. Note in passing that $(\chi_0[Ne_2]|\chi_v[2\,^2\Sigma_u^+ Ne_2^+])_R = \langle\chi_0[Ne_2]|\chi_v[2\,^2\Sigma_u^+ Ne_2^+]\rangle_R$ and $(\chi_v[2\,^2\Sigma_u^+ Ne_2^+]|\Gamma^{1/2}[2\,^2\Sigma_u^+ Ne_2^+](R)|\chi_{E_f}[Ne_2^{2+}])_R = \langle\chi_{E_f}[Ne_2^{2+}]|\Gamma^{1/2}[2\,^2\Sigma_u^+ Ne_2^+](R)|\chi_v[2\,^2\Sigma_u^+ Ne_2^+]\rangle_R$, since in our calculations $\chi_0[Ne_2]$ and $\chi_{E_f}[Ne_2^{2+}]$ are real eigenfunctions of Hermitian Hamilton operators.

$\sigma(E_{\text{kin}})$ is proportional to the probability that an ICD electron with kinetic energy E_{kin} is emitted in the relaxation process of cationic Ne dimer in the $2\,^2\Sigma_u^+$ state. In the following we refer to σ as ''kinetic energy distribution'' or ''spectrum'' of the ICD electrons.

B. Technical comments

The results we obtained by the use of non-Hermitian quantum mechanics could be obtained, of course, also within the framework of the Hermitian approach to quantum mechanics. The numerical advantage in using the time-independent non-Hermitian quantum scattering theory is clear. It enables us to use the adiabatic approximation (with complex potential energy curve) although autoionization takes place and the Born–Oppenheimer approximation developed for Hermitian quantum mechanics is not applicable.

Still, the expression we obtained for the half collision process, $\sigma(E_{\text{kin}})$, describes the preparation of a nuclear wave packet on the *complex* potential energy surface of the cationic neon dimer intermediate. This prepared wave packet is propagated via the nuclear adiabatic cationic dimer Hamiltonian with the complex potential $E[2\,^2\Sigma_u^+ Ne_2^+](R)$. The cationic neon dimer undergoes autoionization resulting in a dicationic neon dimer in a dissociative state.

In our numerical calculations we used the spectral representation of the Green operator where the eigenfunctions of the complex non-Hermitian Hamiltonian have been used as basis functions. These autoionizing vibrational and dissociative eigenfunctions were obtained from complex variational calculations using 900 particle-in-a-box basis functions. The box size in our calculation was 10.6 Å. All matrix elements were calculated by using the accurate numerical integration procedure derived by Harris et al.,[29] which has been shown by Dickinson and Certain to be equivalent to Gaussian quadrature.[30]

IV. FINGERPRINTS OF THE NODAL STRUCTURE OF THE VIBRATIONAL AUTOIONIZING RESONANCE STATES OF $Ne_2^+(2s)$ IN THE KINETIC ENERGY DISTRIBUTIONS

In Fig. 3 we represent our results for the complex eigenvalues, $E_v[2\,^2\Sigma_u^+ Ne_2^+]$. As one can see, the eigenvalues of the nuclear Hamiltonian are divided into two groups. One group is associated with the 11 vibrational autoionizing resonance states. Their characteristic energy spacings are of the order of 10 meV, the typical decay width is about 1 meV. The second group is associated with the dissociative autoionizing resonance states. The discreteness of the dissociative part of the spectrum is due to the use of the finite box approximation in our numerical calculations. We assured of course that our final results for σ are converged in all significant figures. It is interesting to notice that the dissociative autoionizing states form a branch cut of resonances (see Fig. 3), as in the case of electron scattering from the hydrogen molecule.[26] In the latter case the lifetime of the autoionizing states is sufficiently small, such that the branch cut of resonances leads to interference phenomena which make the structure in the cross section be most pronounced.

As we have argued previously, in an ionization experiment each of the resonances shown in Fig. 3 is populated according to its Franck–Condon overlap with the vibrational ground state wave function $\chi_0[Ne_2]$ of the neutral neon dimer. The resulting distribution of the population of the different resonance states is displayed in Fig. 4. Notice that only the vibrational autoionizing states are significantly populated. The ninth vibrational autoionizing state has the largest overlap with $\chi_0[Ne_2]$ and is referred to in the following as ''most populated resonance'' (MPR).

The wave packet on the cationic inner-valence surface of the neon dimer resulting from the population of the vibrational autoionizing states decays by electron emission. However, in order to illustrate the underlying physics of this process, we treat the decay of a single excited vibrational autoionizing state first. This will help to illuminate the more complex behavior of the entire wave packet. As an illustra-
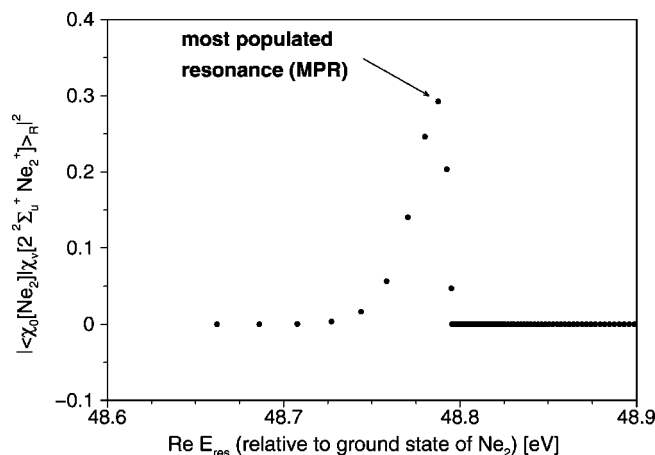
FIG. 4. The Franck–Condon overlaps of the vibrational ground state wave function χ_0 of Ne_2 and the complex vibrational wave functions χ_v of the decaying $2\,^2\Sigma_u^+$ electronic state of Ne_2^+.

tive example we have selected the MPR wave function, though the conclusions which can be drawn are not restricted to this particular choice.

In Fig. 5 we show the structure of the MPR wave function, $|\Psi_{MPR}[2\,^2\Sigma_u^+ Ne_2^+]|^2$, and the kinetic energy distribution, σ_{MPR}, of the ICD electron resulting from the decay of the MPR state. An eye-catching feature of this figure is the fact that the nodal structure in σ_{MPR} reflects the structure in $|\Psi_{MPR}[2\,^2\Sigma_u^+ Ne_2^+]|^2$. There is a one-to-one mapping of the peaks and nodes of the vibrational wave function onto the
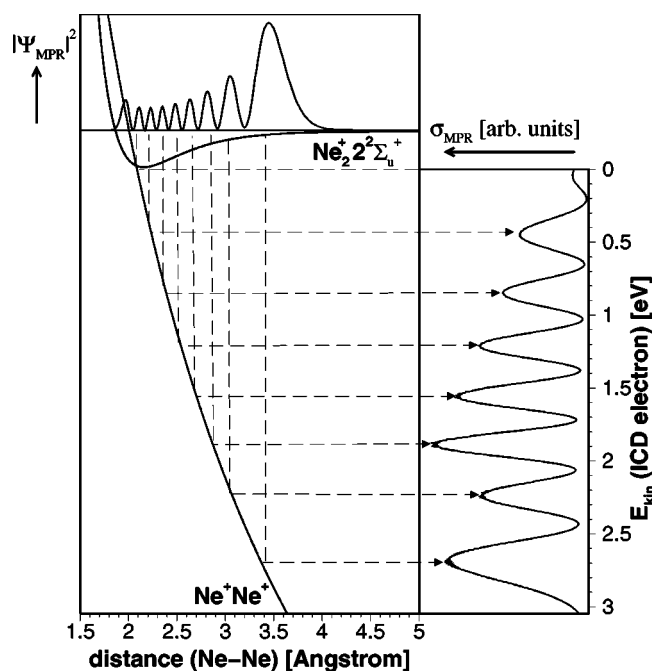

FIG. 5. Mapping of the peaks and nodes of the vibrational resonance wave function (here the most populated vibrational resonance MPR) onto the kinetic energy spectrum (σ_{MPR}) of the ICD electron. Note that there are two factors magnifying the mapping. First, because of the weak bonding in clusters the potential curve of the decaying state is shallow and hence the wave function is extended in coordinate space. Second, because of the two-site nature of the final dicationic state, the corresponding potential curve is steep.

kinetic energy spectrum of the ICD electron. Since the local decay rate $\Gamma[2\,^2\Sigma_u^+ Ne_2^+]$ is a nonconstant function of the interatomic distance, the relative peak heights of $|\Psi_{MPR}[2\,^2\Sigma_u^+ Ne_2^+]|^2$ are modulated under the mapping onto the ICD energy space. The finding that the mapping is not complete and the number of peaks in the wave function is not equal to the number of peaks in the ICD spectrum is due to the fact that the $2\,^2\Sigma_u^+ Ne_2^+$ and the Ne_2^{2+} electronic potential energy curves cross at $R\approx 2.1$ Å. This crossing marks the electron emission threshold. Below this interatomic distance electron emission is energetically not possible. This leads to an abrupt truncation of the ICD electron kinetic energy distribution.

The reflection of the autoionizing vibrational structure in the ICD spectrum should be distinguished from the well-known reflection phenomenon.[31] A structure in the cross section has been observed in photodissociation of molecules where a molecule in its ground electronic but vibrational excited bound state (i.e., nonautoionizing and nonpredissociative state) is excited to a repulsive electronic state which does not support any bound vibrational states. The structure is understood by using the Franck–Condon approximation.[31]

The mapping in the ICD process is particularly spectacular because the nodal structure of the vibrational wave function is magnified onto an electron volt scale. The typical spacing between peaks in the ICD spectrum is about 0.5 eV! Measuring the kinetic energy distribution of the ICD electron would therefore allow the experimentalist to investigate details of vibrational autoionizing states with high resolution. This distinct magnification effect is based on two factors. First, the cationic inner-valence surface is rather flat, thus leading to spatially extended eigenstates. Second, these wave functions are mapped via the dicationic final state curves, which are very steep due to the Coulombic $1/R$ behavior (see Fig. 5).

One possibility to selectively prepare a single vibrational resonance was already mentioned previously, by resonant one-photon excitation from, for example, the $1\,^2\Pi_g$ state of Ne_2^+. Another approach is based on an ionization experiment on the neutral Ne dimer. By measuring the kinetic energy of the photoelectron ejected from the inner-valence with a resolution high enough to distinguish between individual autoionizing vibrational states, one can select one of these and measure the kinetic energy distribution of the corresponding ICD electron in coincidence.

In a standard photoionization experiment, though, not only a single vibrational resonance is populated. As we have already shown in Fig. 4, several resonance states have a significant overlap with the vibrational ground state wave function of neutral Ne_2. Figure 6 depicts the ICD spectrum resulting from the individual contributions of each autoionizing vibrational state weighted by its respective Franck–Condon factor. This spectrum would be obtained if the system under consideration were exposed to a time-dependent noise leading to fast randomly fluctuating phases of the different vibrational and dissociative autoionizing resonances. Thus the quantum interference of these states would be destroyed. It is out of the scope of this work to design such a noise. However, we took its effect into consid-
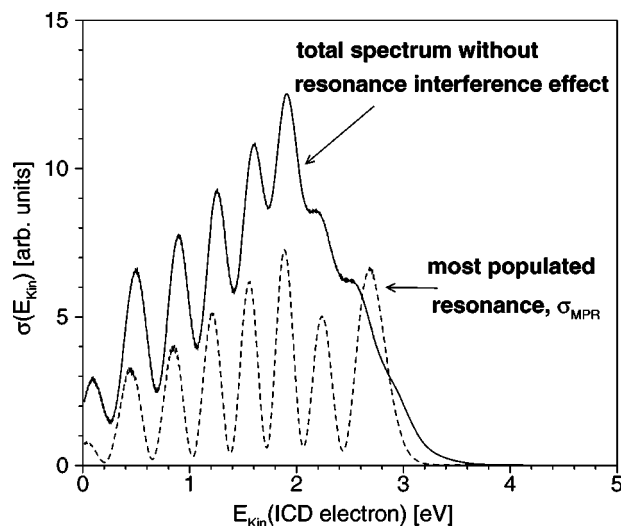
FIG. 6. The spectrum of the kinetic energy of the ICD electron computed without taking into account the interference effects of the vibrational resonances. Also shown is the spectrum σ_{MPR} of the most populated resonance. σ_{MPR} is the spectrum obtained if only one (the MPR) vibrational resonance is initially excited.

eration by taking the sum of the absolute values of the contributions of the resonances to σ rather than by taking the absolute value of the sum [see Eq. (6)]. As one can see from Fig. 6, the total ICD spectrum without resonance interference effects possesses the same pronounced structure as that spectrum which is obtained from the sole contribution of the most populated vibrational resonance (MPR). This marked structure is a manifestation of the nodal pattern of the resonances underlying the vibrational wave packet on the $2\ ^2\Sigma_u^+$ surface of Ne_2^+.

If the coherence of this wave packet is conserved during the experiment, Eq. (6) can be applied directly and the kinetic energy distribution of the ICD electron looks as displayed in Fig. 7. By analyzing Eq. (6) in detail it is possible to show that for large decay widths the ICD spectrum is basically identical to the Gaussian-type wave packet result-
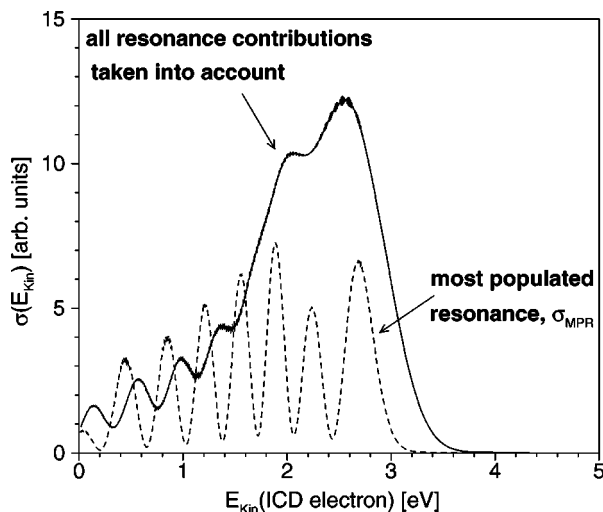
FIG. 7. The kinetic energy spectrum of the ICD electron. Here, all interference effects of the vibrational resonances are taken into account.

ing from the initial ionization process. In the neon dimer, however, there is a strong competition between electronic decay and nuclear dynamics, i.e., both take place on the same time scale. Therefore, indications for the Gaussian-type wave packet in the ICD spectrum are noticeable only in the kinetic energy range between 2.5 and 4 eV. At lower kinetic energies a nodal structure is visible, which can again be attributed to the features of the excited autoionizing vibrational states.

In fact, due to nonlocal effects not included in Eq. (6), the experimentally observed ICD spectrum should be expected to possess an even more pronounced and complicated structure at low kinetic energies. The Rydberg state surfaces of Ne_2^+ converging to the repulsive dicationic potential energy surface support dissociating autoionizing states. In the local picture the corresponding width functions $\Gamma(R)$ vanish. In reality, however, because energy can be transferred between nuclear and electronic motion, the resulting Rydberg states can electronically decay. These dissociative resonances can interact with a vibrational resonance on the $2\ ^2\Sigma_u^+$ surface if their total energy is equal to that of the latter state. In analogy to other dissociative processes, the coupling is non-negligible only in the vicinity of the dicationic final state surface. This can be understood by reference to Fig. 5. The Rydberg state surfaces under consideration are essentially parallel to the steep repulsive dicationic surface which they converge to. Such dissociative Rydberg states are characterized by quickly oscillating nuclear wave functions. Only close to the dicationic final state surface are the oscillations slow enough to give rise to appreciable interaction with a vibrational resonance on the inner-valence surface. A similar argument applies to the coupling of these Rydberg states to those states associated with two dissociating Ne^+ fragments and a free electron. As a consequence, the Rydberg states can decay, but only by emission of an electron close to threshold, i.e., with basically zero kinetic energy.

In an experiment it might be easier to observe the reflection of the nodal structure of the autoionizing vibrational wave functions of $2\ ^2\Sigma_u^+\ Ne_2^+$ in the spectrum by measuring the kinetic energy distribution of the Ne^+ fragments rather than measuring the ICD electron kinetic energy distribution. Such a technique was already successfully employed by Thissen et al.[32] for investigating the energy transfer process in inner-valence ionized rare gas dimers. We calculated the kinetic energy distribution of the Ne^+ fragments, $\tilde{\sigma}(E_f)$, by replacing the integration (i.e., summation in our numerical calculations) over the final vibrational state energies E_f in Eq. (6) by the integration over the kinetic energy E_{kin} of the ICD electron. In Fig. 8 we represent our results for $\tilde{\sigma}(E_f)$. In order to compare these to the kinetic energy distribution of the ICD electron discussed previously, one should note that both kinetic energy spectra are basically complementary. If an ICD electron is emitted at an internuclear distance only slightly larger than the curve crossing point at $R \approx 2.1$ Å, its kinetic energy is necessarily almost zero. On the other hand, because of the steep dicationic potential energy curve, the kinetic energy of the Ne^+ fragments is at its maximum in this case. Taking this into account we subtracted the kinetic energy of the Ne^+ fragments from the maximum value this
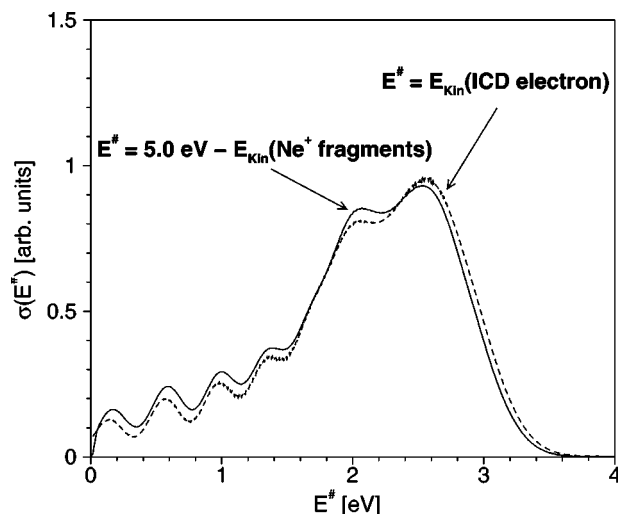
FIG. 8. The spectrum of the kinetic energy of the Ne$^+$ fragments after Coulomb explosion (solid line) compared to the spectrum of the ICD electron (broken line). Note the shifted energy scale of the fragments' kinetic energy (see the text).

observable assumes (5.0 eV). As can be seen in Fig. 8, the structure found in the emission spectrum of the ICD electron is present also in the kinetic energy spectrum of the Ne$^+$ fragments.

V. CONCLUDING REMARKS

In this paper we have investigated in detail the relaxation behavior of the van der Waals system neon dimer following inner-valence ionization. We have shown that an interatomic electronic decay (ICD) takes place, which is a manifestation of an efficient energy transfer between Ne$^+(2s)$ and Ne. The relevant potential energy surfaces of Ne$_2$, Ne$_2^+$, and Ne$_2^{2+}$ have been presented as well as the electronic decay width for the $2\,^2\Sigma_u^+$ inner-valence state of Ne$_2^+$. Electron emission and dynamics of the atomic nuclei have been found to take place on comparable time scales, which are of the order of 100 fs. Using non-Hermitian quantum scattering theory we calculated the kinetic energy distributions of Ne$^+$ and of the free ICD electron that result after an inner-valence electron has been removed from the neutral neon dimer in its ground vibrational and electronic state. The essential point to note here is the interatomic Coulombic character of this electronic decay process. We have shown that there is a pronounced structure in the kinetic energy distributions of the ICD electron as well as of the Ne$^+$ fragments which reflects the nodal vibrational structure of the autoionizing state of the electronically excited cationic neon dimer. The peaks in the kinetic energy distributions are separated by a relatively large energy of approximately 0.5 eV compared to the vibrational energy spacings of about 10 meV in the decaying states. Both the Coulombic explosion of Ne$_2^{2+}$ and the soft mode nature (i.e., close to dissociation) of the metastable autoionizing states of Ne$_2^+(2s)$ act as magnifying factors in this mapping process. Because of this magnification, the kinetic energy distributions studied are very sensitive to details of

the underlying electronic potential energy curve of the decaying state in the cluster. We hope that our results will stimulate experiments.

We would like to emphasize that interesting results are also expected for larger clusters. In those systems the lifetime of the electronic autoionizing states of the cationic clusters is predicted to be smaller than in dimers.[4] Due to the enhanced lifetime broadening the vibrational autoionizing states will energetically overlap stronger than in the dimer, and this is expected to give rise to more pronounced interference effects. We also anticipate an increase of the coupling between the electronic and nuclear motions as the size of the cluster is increased. The interplay of shorter lifetimes and larger electronic–nuclear couplings may cause the appearance of further interesting phenomena like dynamical trapping of the ICD electron at specific energies.

APPENDIX: KINETIC ENERGY DISTRIBUTIONS

Equation (6) has been derived on the basis of the non-Hermitian scattering theory developed by Moiseyev and co-workers. In this paper we have demonstrated a novel application of this technique, namely, to the reaction

$$\text{Ne}_2 + \hbar\omega \rightarrow [\text{Ne}_2^+]^* + e^- \rightarrow [\text{Ne}_2^{2+} + e^-(\text{ICD})] + e^-$$
$$\rightarrow 2\text{Ne}^+ + 2e^-,$$
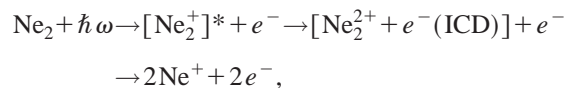
where the electronically excited cationic dimer, $[\text{Ne}_2^+]^*$, has a hole in its inner-valence $2s$-type molecular orbital $2\,^2\Sigma_u^+$. For the sake of clarity and completeness we present in this Appendix the derivation of the expressions for the kinetic energy distributions of the emitted ICD electron and of the Ne$^+$ fragments.

Within the framework of the Born–Oppenheimer (BO) approximation the initial state, that is, the ground state of neutral neon dimer, is given by

$$\Psi_0[\text{Ne}_2](\{\mathbf{r}\}_N, R) = \psi^{\text{elec}}[\text{Ne}_2](\{\mathbf{r}\}_N; R)\chi_0[\text{Ne}_2](R).$$
$$(A1)$$

$N = 20$ is the number of electrons, $\{\mathbf{r}\}_N$ is the notation for the coordinates of the N electrons, $\psi^{\text{elec}}[\text{Ne}_2]$ is the adiabatic electronic wave function in the electronic ground state of Ne$_2$, and $\chi_0[\text{Ne}_2]$ is the vibrational eigenfunction of the nuclear Hamiltonian with the electronic ground state potential energy surface.

Utilizing electromagnetic radiation from a synchrotron source, for instance, an inner-valence electron can be ejected and a superposition of autoionizing states of Ne$_2^+$ in the $2\,^2\Sigma_u^+$ electronic state is generated. We can approximate

these resonance states by the BO solutions only when the non-Hermitian approach is taken and the potential energy surface obtained from the electronic structure calculations is complex, $E[2\,^2\Sigma_u^+ \mathrm{Ne}_2^+](R) = \mathrm{Re}\,E[2\,^2\Sigma_u^+ \mathrm{Ne}_2^+](R) - (i/2)\Gamma[2\,^2\Sigma_u^+ \mathrm{Ne}_2^+](R)$. Under these circumstances the autoionizing states of $[\mathrm{Ne}_2^+]^*$ can be factorized into an electronic and a nuclear part,

$$
\begin{aligned}
&\Psi_v[2\,^2\Sigma_u^+ \mathrm{Ne}_2^+](\{\mathbf{r}\}_{N-1}, R) \\
&= \psi^{\mathrm{elec}}[2\,^2\Sigma_u^+ \mathrm{Ne}_2^+](\{\mathbf{r}\}_{N-1}, R)\chi_v[2\,^2\Sigma_u^+ \mathrm{Ne}_2^+](R).
\end{aligned}
$$
(A2)

Exposing Ne_2 to radiation with photon energy $\hbar\omega$ significantly above the inner-valence ionization threshold can lead to formation of a wave packet of the $(N-1)$-electron system $[\mathrm{Ne}_2^+]^*$,

$$
\begin{aligned}
&\Phi^{\mathrm{WP}}[2\,^2\Sigma_u^+ \mathrm{Ne}_2^+](\{\mathbf{r}\}_{N-1}, R) \\
&= \sum_v\,(\chi_v[2\,^2\Sigma_u^+ \mathrm{Ne}_2^+]|\mu(R)|\chi_0[\mathrm{Ne}_2])_R \\
&\quad\times \Psi_v[2\,^2\Sigma_u^+ \mathrm{Ne}_2^+](\{\mathbf{r}\}_{N-1}, R),
\end{aligned}
$$
(A3)

and a photoelectron in state ϕ_{PE}, which in the sudden approximation does not interact with the Ne_2^+ cation. Thus the dipole transition moment $\mu(R)$ is given by

$$
\mu(R) = \left(\mathcal{A}\{\psi^{\mathrm{elec}}[2\,^2\Sigma_u^+ \mathrm{Ne}_2^+]\phi_{\mathrm{PE}}\} \middle| e\sum_{i=1}^N \mathbf{r}_i\cdot\mathbf{e}_z \middle| \psi^{\mathrm{elec}}[\mathrm{Ne}_2] \right)_{\mathbf{r}},
$$
(A4)

where $(\cdot|\cdot)_{\mathbf{r}}$ indicates integration over the electronic coordinates, e denotes the charge of an electron, and $\mathbf{e}_z$ is a unit vector along the polarization axis of linearly polarized light. The symbol $\mathcal{A}$ is used to emphasize that the product state of cation and photoelectron must be properly antisymmetrized.

The wave packet $\Phi^{\mathrm{WP}}[2\,^2\Sigma_u^+ \mathrm{Ne}_2^+]$ undergoes electronic decay according to the ICD mechanism. The products of this relaxation process are dissociative Ne_2^{2+} in its electronic ground state and a free ICD electron in state ϕ_{ICD} with kinetic energy E_{kin}. Within the framework of the BO approximation the final states can be written as

$$
\begin{aligned}
&\Psi_f[\mathrm{Ne}_2^{2+} + e^-(\mathrm{ICD})](\{\mathbf{r}\}_{N-1}, R) \\
&= \mathcal{A}\{\phi_{\mathrm{ICD}}\psi^{\mathrm{elec}}[\mathrm{Ne}_2^{2+}]\}(\{\mathbf{r}\}_{N-1}; R)\chi_{E_f}[\mathrm{Ne}_2^{2+}](R).
\end{aligned}
$$
(A5)

The dissociative nuclear wave functions $\chi_{E_f}[\mathrm{Ne}_2^{2+}]$ are associated with continuous energies $E_f[\mathrm{Ne}_2^{2+}]$. Therefore the energy of the state $\Psi_f[\mathrm{Ne}_2^{2+} + e^-(\mathrm{ICD})]$ is $E_{\mathrm{kin}} + E_f[\mathrm{Ne}_2^{2+}]$.

We treat the coupling between the ICD electron and the dication by means of the Lippmann–Schwinger equation extended to non-Hermitian Hamiltonians:

$$
\begin{aligned}
\Phi_f[\mathrm{Ne}_2^+] &= (1 + \hat{G}(E_{\mathrm{kin}} + E_f[\mathrm{Ne}_2^{2+}])\hat{V}) \\
&\quad\times \Psi_f[\mathrm{Ne}_2^{2+} + e^-(\mathrm{ICD})].
\end{aligned}
$$
(A6)

$(\Phi^{\mathrm{WP}}[2\,^2\Sigma_u^+ \mathrm{Ne}_2^+]|\Phi_f[\mathrm{Ne}_2^+])$ is the probability amplitude that the wave packet $\Phi^{\mathrm{WP}}[2\,^2\Sigma_u^+ \mathrm{Ne}_2^+]$ decays into Ne_2^{2+} with energy $E_f[\mathrm{Ne}_2^{2+}]$ and an ICD electron with energy E_{kin}. The expression explicitly reads

$$
(\Phi^{\mathrm{WP}}[2\,^2\Sigma_u^+ \mathrm{Ne}_2^+]|\Phi_f[\mathrm{Ne}_2^+]) = \sum_v \frac{(\chi_0[\mathrm{Ne}_2]|\mu(R)|\chi_v[2\,^2\Sigma_u^+ \mathrm{Ne}_2^+])_R (\Psi_v[2\,^2\Sigma_u^+ \mathrm{Ne}_2^+]|\hat{V}|\Psi_f[\mathrm{Ne}_2^{2+} + e^-(\mathrm{ICD})])_{\mathbf{r},R}}{E_{\mathrm{kin}} + E_f[\mathrm{Ne}_2^{2+}] - E_v[2\,^2\Sigma_u^+ \mathrm{Ne}_2^+]}.
$$
(A7)

What remains to be discussed is the determination of the interaction matrix elements $(\Psi_v[2\,^2\Sigma_u^+ \mathrm{Ne}_2^+]|\hat{V}|\Psi_f[\mathrm{Ne}_2^{2+} + e^-(\mathrm{ICD})])_{\mathbf{r},R}$. $\hat{V}$ is defined as

$$
\hat{V} = \hat{H}[2\,^2\Sigma_u^+ \mathrm{Ne}_2^+] - \hat{H}[\mathrm{Ne}_2^{2+} + e^-(\mathrm{ICD})].
$$
(A8)

As explained in the text, $\hat{H}[2\,^2\Sigma_u^+ \mathrm{Ne}_2^+]$ is a complex, non-Hermitian Hamiltonian whereas $\hat{H}[\mathrm{Ne}_2^{2+} + e^-(\mathrm{ICD})]$ is Hermitian. By using the BO expressions for $\Psi_v[2\,^2\Sigma_u^+ \mathrm{Ne}_2^+]$ [Eq. (A2)] and $\Psi_f[\mathrm{Ne}_2^{2+} + e^-(\mathrm{ICD})]$ [Eq. (A5)] it is straightforward to derive that

$$
\begin{aligned}
&(\Psi_v[2\,^2\Sigma_u^+ \mathrm{Ne}_2^+]|\hat{V}|\Psi_f[\mathrm{Ne}_2^{2+} + e^-(\mathrm{ICD})])_{\mathbf{r},R} \\
&= (\chi_v[2\,^2\Sigma_u^+ \mathrm{Ne}_2^+]|d(R)|\chi_{E_f}[\mathrm{Ne}_2^{2+}])_R,
\end{aligned}
$$
(A9)

where

$$
d(R) = (\psi^{\mathrm{elec}}[2\,^2\Sigma_u^+ \mathrm{Ne}_2^+]|\hat{V}|\mathcal{A}\{\phi_{\mathrm{ICD}}\psi^{\mathrm{elec}}[\mathrm{Ne}_2^{2+}]\})_{\mathbf{r}}.
$$
(A10)

Moiseyev and co-workers have shown[22,33] that, apart from a multiplicative constant, in the local approximation

$$
d(R) = e^{i\varphi(R)}\sqrt{\Gamma(R)}.
$$
(A11)

Here $\Gamma(R) = \Gamma[2\,^2\Sigma_u^+ \mathrm{Ne}_2^+](R)$ is the local electronic decay width of inner-valence ionized neon dimer and $\varphi(R)$ is the phase of the resonance width amplitude.

The kinetic energy distribution of the ICD electrons, $\sigma(E_{\mathrm{kin}})$, is obtained by adding up all decay probabilities $|(\Phi^{\mathrm{WP}}[2\,^2\Sigma_u^+ \mathrm{Ne}_2^+]|\Phi_f[\mathrm{Ne}_2^+])|^2$ that are associated with an ICD electron of energy E_{kin} in the final state,

$$
\sigma(E_{\mathrm{kin}}) = \int dE_f[\mathrm{Ne}_2^{2+}]|(\Phi^{\mathrm{WP}}[2\,^2\Sigma_u^+ \mathrm{Ne}_2^+]|\Phi_f[\mathrm{Ne}_2^+])|^2.
$$
(A12)

Assuming $\mu(R) = 1$ and $\varphi(R) = 1$, Eq. (6) follows immediately by inserting Eqs. (A7), (A9), and (A11) into Eq. (A12). In a similar fashion the kinetic energy distribution of the Ne^+ fragments, $\tilde{\sigma}(E_f)$, is given by

$$
\tilde{\sigma}(E_f) = \int dE_{\mathrm{kin}}|(\Phi^{\mathrm{WP}}[2\,^2\Sigma_u^+ \mathrm{Ne}_2^+]|\Phi_f[\mathrm{Ne}_2^+])|^2.
$$
(A13)

[1] M. Thompson, M. D. Baker, A. Christie, and J. F. Tyson, *Auger Electron Spectroscopy* (Wiley, New York, 1985).

[2] L. S. Cederbaum, J. Zobeley, and F. Tarantelli, Phys. Rev. Lett. **79**, 4778 (1997).

[3] J. Zobeley, L. S. Cederbaum, and F. Tarantelli, J. Chem. Phys. **108**, 9737 (1998).

[4] R. Santra, J. Zobeley, L. S. Cederbaum, and N. Moiseyev, Phys. Rev. Lett. **85**, 4490 (2000).

[5] J. Zobeley, L. S. Cederbaum, and F. Tarantelli, J. Phys. Chem. A **103**, 11145 (1999).

[6] J. Schirmer, L. S. Cederbaum, and O. Walter, Phys. Rev. A **28**, 1237 (1983).

[7] J. Schirmer and A. Barth, Z. Phys. A **317**, 267 (1984).

[8] F. O. Gottfried, L. S. Cederbaum, and F. Tarantelli, Phys. Rev. A **53**, 2118 (1996).

[9] L. S. Cederbaum, in *Encyclopedia of Computational Chemistry*, edited by P. v. R. Schleyer *et al.* (Wiley, New York, 1998).

[10] GAMESS-UK is a package of *ab initio* programs written by M. F. Guest, J. H. van Lenthe, J. Kendrick, K. Schoffel, and P. Sherwood, with contributions from R. D. Amos, R. J. Buenker, H. J. J. van Dam, M. Dupuis, N. C. Handy, I. H. Hillier, P. J. Knowles, V. Bonacic-Koutecky, W. von Niessen, R. J. Harrison, A. P. Rendell, V. R. Saunders, A. J. Stone, and A. H. de Vries. The package is derived from the original GAMESS code due to M. Dupuis, D. Spangler, and J. Wendoloski, NRCC Software Catalog, Vol. 1, Program No. QG01 (GAMESS) (1980).

[11] D. E. Woon and T. H. Dunning, Jr., J. Chem. Phys. **100**, 2975 (1994). Basis sets were obtained from the Extensible Computational Chemistry Environment Basis Set Database, Version 1.0, as developed and distributed by the Molecular Science Computing Facility, Environmental and Molecular Sciences Laboratory which is part of the Pacific Northwest Laboratory, P.O. Box 999, Richland, WA 99352, and funded by the U.S. Department of Energy. The Pacific Northwest Laboratory is a multiprogram laboratory operated by Battelle Memorial Institute for the U.S. De-

partment of Energy under Contract No. DE-AC06-76RLO 1830.

[12] T. van Mourik, A. K. Wilson, and T. H. Dunning, Jr., Mol. Phys. **96**, 529 (1999).

[13] J. Mášik, J. Urban, P. Mach, and I. Hubač, Int. J. Quantum Chem. **63**, 333 (1997).

[14] T. Sommerfeld, U. V. Riss, H.-D. Meyer, L. S. Cederbaum, B. Engels, and H. U. Suter, J. Phys. B **31**, 4107 (1998).

[15] R. Santra, L. S. Cederbaum, and H.-D. Meyer, Chem. Phys. Lett. **303**, 413 (1999).

[16] U. V. Riss and H.-D. Meyer, J. Phys. B **26**, 4503 (1993).

[17] A. Szabo and N. S. Ostlund, *Modern Quantum Chemistry* (Dover, Mineola, 1996).

[18] E. P. Wigner, Phys. Rev. **73**, 1002 (1948).

[19] W. Domcke, Phys. Rep. **208**, 97 (1991).

[20] P. Lablanquie *et al.*, Phys. Rev. Lett. **84**, 431 (2000).

[21] N. Moiseyev, Phys. Rep. **302**, 211 (1998).

[22] E. Narevicius and N. Moiseyev, J. Chem. Phys. **113**, 6088 (2000).

[23] J. R. Taylor, *Scattering Theory* (Wiley, New York, 1972).

[24] N. Moiseyev, J. Phys. B **31**, 1431 (1998).

[25] *The Letropet Symposium View on a Generalized Inner Product*, edited by E. Brändas and N. Elander, Lecture Notes in Physics, Vol. 325 (Springer, Berlin, 1998).

[26] E. Narevicius and N. Moiseyev, Phys. Rev. Lett. **84**, 1681 (2000).

[27] L. S. Cederbaum and W. Domcke, J. Phys. B **14**, 4665 (1981).

[28] L. S. Cederbaum and W. Domcke, Adv. Chem. Phys. **36**, 205 (1977).

[29] D. O. Harris, H. W. Harrington, A. L. Luntz, and W. P. Gwinn, J. Chem. Phys. **44**, 3467 (1966).

[30] A. S. Dickinson and P. R. Certain, J. Chem. Phys. **49**, 4209 (1968).

[31] R. Schinke, *Photodissociation Dynamics* (Cambridge University Press, Cambridge, 1993), pp. 316–319.

[32] R. Thissen, P. Lablanquie, R. I. Hall, M. Ukai, and K. Ito, Eur. Phys. J. D **4**, 335 (1998).

[33] N. Moiseyev and U. Peskin, Phys. Rev. A **42**, 255 (1990).